Characterization of Nitrosoalkane Binding and Activation of Soluble Guanylate Cyclase†

Emily R. Derbyshire,‡ Rosalie Tran,§ Richard A. Mathies,§,|| and Michael A. Marletta*,‡,§,||

Department of Molecular and Cell Biology, Department of Chemistry, and Division of Physical Biosciences, Lawrence Berkeley National Laboratory, University of California, Berkeley, California 94720-1460

Received August 7, 2005; Revised Manuscript Received October 6, 2005

ABSTRACT: Soluble guanylate cyclase (sGC) is the primary receptor for the signaling agent nitric oxide (NO). Electronic absorption and resonance Raman spectroscopy were used to show that nitrosoalkanes bind to the heme of sGC to form six-coordinate, low-spin complexes. In the sGC−nitrosopentane complex, a band assigned to an Fe−N stretching vibration is observed at 543 cm^{-1} which is similar to values reported for other six-coordinate NO-bound hemoproteins. Nitrosoalkanes activate sGC 2−6-fold and synergize with YC-1, a synthetic benzylindazole derivative, to activate the enzyme 11−47-fold. In addition, the observed off-rates of nitrosoalkanes from sGC were found to be dependent on the alkyl chain length. A linear correlation was found between the observed off-rates and the alkyl chain length which suggests that the sGC heme has a large hydrophobic distal ligand-binding pocket. Together, these data show that nitrosoalkanes are a novel class of heme-based sGC activators and suggest that heme ligation is a general requirement for YC-1 synergism.

Soluble guanylate cyclase (sGC)[1] is the primary nitric oxide (NO) receptor in mammals. sGC catalyzes the synthesis of the second messenger cyclic guanosine 3′,5′-monophosphate (cGMP) from guanosine 5′-triphosphate (GTP). cGMP is critical to several signaling pathways, including those that regulate vascular smooth muscle relaxation, neuronal signaling, and platelet aggregation (*1*−*4*). An understanding of the mechanism of sGC activation is important in the rational design of therapeutic agents for treating diseases involving the NO−cGMP pathway.

sGC is a heterodimeric hemoprotein that consists of two homologous subunits, α and *β*. The heme-binding domain of sGC has been localized to the N-terminus of the *β*1 subunit where the heme cofactor is ligated by histidine 105 (*5*, *6*). Constructs containing the isolated domains, *β*1(1−385)[2] and *β*1(1−194), have heme binding properties similar to those of the heterodimeric protein (*7*, *8*). The catalytic domains are localized to the C-terminus of each subunit. The isolated catalytic domains from each subunit have been expressed, purified, and shown to dimerize and catalyze the production of cGMP (*9*).

The integration of the sGC sensor domain and the catalytic domains with regard to global structure and the sGC mechanism of activation are largely unknown. There are two primary ways to fully activate sGC *in vitro*: using NO or NO donors, or the combination of carbon monoxide (CO) and YC-1. The interaction of NO with the sGC heme causes the proximal Fe−His bond to break, leading to a five-coordinate heme−nitrosyl complex, coincident with a several hundred-fold increase in the extent of activation (*10*, *11*). CO or YC-1 alone activates the enzyme 4−11-fold (*10*, *12*), but they synergistically activate sGC several hundred-fold (*13*, *14*). While the breaking of the Fe−His bond has been thought to be solely responsible for activation, the high activity of the six-coordinate sGC−CO complex in the presence of YC-1 suggests that a five-coordinate sGC complex is not essential for full activation. Details of the mechanism of activation by NO and by CO or YC-1 remain to be elucidated.

Novel ligands that bind to the sGC heme and/or activate the enzyme can yield information about the sGC heme pocket and expand our understanding of the mechanism of sGC. Nitrosoalkanes (RNO) are a potential class of sGC heme ligands. These compounds are well-characterized ligands for myoglobin and hemoglobin (*15*, *16*), and are particularly interesting for studies with sGC because they are essentially alkyl-substituted NO compounds (Figure 1). Previously, nitrosomethane was shown to bind to the heme of sGC (*17*), but the relatively fast off-rate of the ligand under the conditions that were used prevented further characterization. Here, we show that by increasing the alkyl chain length of nitrosoalkanes, a stable sGC−nitrosoalkane complex can be formed. Using electronic absorption and resonance Raman

† Funding was provided by the LDRD from LBNL, the DeBenedictis Fund to M.A.M., and Grant T32 GM07232 to E.R.D.

* To whom correspondence should be addressed: Department of Chemistry, 211 Lewis Hall, University of California, Berkeley, CA 94720-1460. Phone: (510) 643-9325. Fax: (510) 643-9388. E-mail: marletta@berkeley.edu.

‡ Department of Molecular and Cell Biology.

§ Department of Chemistry.

|| Division of Physical Biosciences.

[1] Abbreviations: sGC, soluble guanylate cyclase; NO, nitric oxide; GTP, guanosine 5′-triphosphate; cGMP, cyclic guanosine 3′,5′-monophosphate; Hb, hemoglobin; Mb, myoglobin; Sf9, *Spodoptera frugiperda*; DEA/NO, diethylammonium (*Z*)-1-(*N*,*N*-diethylamino)diazen-1-ium-1,2-diolate; YC-1, 3-(5′-hydroxymethyl-3′-furyl)-1-benzylindazole; HEPES, 4-(2-hydroxyethyl)-1-piperazineethanesulfonic acid; EIA, enzyme immunoassay.

[2] sGC amino acid numbering is that of the rat enzyme unless otherwise noted.

10.1021/bi0515671 CCC: $30.25 © 2005 American Chemical Society
Published on Web 11/12/2005

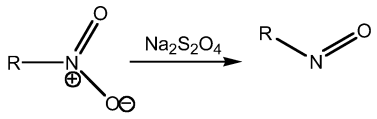

FIGURE 1: Reaction of nitroalkanes (RNO_2) with dithionite ($Na_2S_2O_4$) produces nitrosoalkanes (RNO).

spectroscopy, nitrosoalkanes are shown to bind to the heme of sGC to form six-coordinate, low-spin complexes. At 25 °C, nitrosoalkanes activate sGC 2−6-fold and act synergistically with YC-1 to activate sGC 11−47-fold. YC-1 alone activates sGC 3-fold, while NO activates the enzyme 127-fold. Additionally, a quantitative structure−activity relationship (QSAR) analysis was performed correlating increasing nitrosoalkane alkyl chain length with observed off-rates. The results reveal structural information about the sGC heme distal pocket and provide insight into the mechanism of enzyme activation.

MATERIALS AND METHODS

Materials. sGC was expressed using a baculovirus/Sf9 expression system and purified as described previously (*18*). The sGC heme domain β1(1−194) was prepared according to a protocol which will be described elsewhere (*8*). ^{15}N-labeled sodium nitrite was from Cambridge Isotope Laboratories. Diethylammonium (*Z*)-1-(*N*,*N*-diethylamino)diazen-1-ium-1,2-diolate (DEA/NO) was from Cayman Chemical Co. All other reagents were from Sigma, unless otherwise noted.

Synthesis of [^{15}*N*]*Nitropentane*. 1-Bromopentane (720 mg, 4.8 mmol) was added dropwise to a stirred solution of $Na^{15}NO_2$ (716 mg, 10 mmol) in dimethylformamide (12 mL). The solution was stirred in the dark at room temperature for 40 min. The reaction was stopped by addition of 10 mL of cold water, which was followed by a 3 × 10 mL extraction with diethyl ether. The combined extracts were dried over sodium sulfate and passed through a bed of Florisil and then a bed of silica (*19*). Solvent was removed under vacuum to afford [^{15}N]nitropentane (95% pure) that was used without further purification: ^{1}H NMR ($CDCl_3$/TMS) δ 0.91 (t, 3H, CH_3−), 1.35 (m, 4H, $CH_3-CH_2-CH_2-$), 2.00 (5, 2H, $-CH_2-CH_2NO_2$), 4.36 (t, 2H, $-CH_2NO_2$, J = 1.81 Hz); ^{13}C NMR ($CDCl_3$/TMS) δ 13.99 (CH_3−), 22.22 (CH_3-CH_2-), 27.36 ($-CH_2-CH_2-CH_2-$), 28.55 ($-CH_2-CH_2-NO_2$), 75.97 (CH_2-NO_2, J = 7.52 Hz).

Preparation of Protein−Nitrosoalkane Complexes. Electronic absorption spectra were collected on a CARY 3E spectrophotometer with a Neslab RTE-100 temperature controller set at 25 °C. Spectra were collected over the range of 700−250 nm every 1.5 min at 600 nm/min with a 1 nm data point interval. Stock solutions of 1 M nitromethane, nitropropane, nitrobutane, nitropentane, nitrohexane, and nitrooctane were made in DMSO. Dithionite stock solutions (5 and 0.5 M) in H_2O were prepared in a Teflon-sealed Reacti-Vial (Pierce) using an anaerobic chamber (Coy). Nitrosoalkanes were generated *in situ* by reduction of a specific nitroalkane with dithionite (Figure 1) (*15*, *17*). Nitrosoalkane−sGC complexes were made by addition of 1 μL of 1 M nitroalkane followed by 1 μL of 0.5 M dithionite using a gastight syringe (Hamilton) to 0.5−1 μM purified sGC or β1(1−194) in 50 mM HEPES (pH 7.4) and 100 mM NaCl. The final reaction mixture contained 0.5−1 μM protein, 10 mM nitroalkane, 5 mM dithionite, and 1% DMSO. For horse heart myoglobin (Mb) or human hemoglobin (Hb), 1 μL of 5 M nitroalkane and 1 μL of 5 M dithionite were used to generate the complexes (lower concentrations of reagents would not produce a fully nitrosoalkane-bound heme). The final reaction mixture contained 0.5−1 μM protein, 50 mM nitroalkane, and 50 mM dithionite. Each solution was briefly mixed, and reactions were monitored by following the shift in the Soret absorbance maximum from 431 to 421−425 nm until binding was complete as indicated by the absence of any further spectral change upon addition of excess nitrosoalkane.

Observed Off-Rates of Nitrosoalkanes from sGC. sGC−nitrosoalkane complexes were made as described above. After binding of the nitrosoalkane was complete, excess nitroalkane and dithionite were removed by desalting into 50 mM HEPES (pH 7.4) and 100 mM NaCl by three cycles of dilution and concentration using a 10K Ultrafree-0.5 centrifugal filter device (Millipore). Nitrosoalkane off-rates from sGC (400−600 nM) were monitored by electronic absorption spectroscopy at 25 °C. Spectra of sGC complexes with nitrosopropane were collected every 0.5 min for 60 min over the range of 500−350 nm at 600 nm/min with a 1 nm data point interval. For nitrosobutane−, nitrosopentane−, nitrosohexane−, and nitrosooctane−sGC complexes, spectra were collected every 1 min for 120 min over the range of 700−350 nm at 600 nm/min with a 1 nm data point interval. A buffer baseline [50 mM HEPES (pH 7.4) and 100 mM NaCl] was subtracted from each spectrum, and spectra were corrected for baseline drift by subtracting the average absorbance of 700−690 nm from each spectrum. Difference spectra were obtained by subtraction of a time zero spectrum from all subsequent spectra. ΔA_{438} and ΔA_{423} values were extracted from the difference spectra, and $\Delta A_{438} - \Delta A_{423}$ was plotted versus time for each experiment. The data were fit to a single exponential [$A = A_t(1 - e^{-kt})$] to obtain the observed off-rates. Each experiment was repeated to ensure reproducibility.

Preparation of Resonance Raman Samples. Nitrosoalkane complexes of Mb, β1(1−194), and sGC for resonance Raman spectroscopy were prepared as described above, except that the β1(1−194)−[^{15}N]nitrosopentane complex was made by addition of 25 mM [^{15}N]nitropentane and 5 mM dithionite. The final concentrations of Mb−nitrosomethane and Mb−nitrosopentane complexes were 50 μM. Concentrations of β1(1−194)−[^{14}N]nitrosopentane, β1(1−194)−[^{15}N]nitrosopentane, and β1(1−194)−nitrosomethane complexes were 20 μM, while the concentration of the sGC−nitrosopentane complex was 5 μM. The final volume of all samples was 500 μL in 50 mM HEPES (pH 7.4) and 100 mM NaCl.

Resonance Raman Spectroscopy. Spectra were collected using 413.1 nm excitation from a Kr^+ laser (Spectra-Physics model 2025). Raman scattering was detected with a back-illuminated liquid nitrogen-cooled CCD (LN/CCD-1100/PB, Roper Scientific) controlled by a ST-133 controller coupled to a subtractive dispersion double spectrograph. The laser power at the samples was approximately 2 mW, focused to a 60 μm beam diameter. To minimize degradation of samples, protein in a microspinning sample cell was cooled to 10 °C with a stream of cooled nitrogen gas. Data acquisition times ranged from 50 to 60 min. Spectra were

corrected for the wavelength dependence of the spectrometer efficiency using a white lamp, and the instrument was calibrated using cyclohexane. The reported frequencies are accurate to ± 2 cm^{-1}, and the resolution of the spectra is 8 cm^{-1}. The buffer background signal was subtracted from each Raman spectrum, and the spectra were baseline corrected. An electronic absorption spectrum of the protein was collected after Raman data acquisition was complete to determine whether photo-induced degradation had occurred. There was no change in the Soret or the α/β bands in any of the samples, except for the sGC−nitrosopentane complex, the Soret band appeared to be slightly broader after exposure to the laser. Approximate isotopic shifts were estimated on the basis of a simple diatomic harmonic oscillator model.

sGC Activity. Triplicate end-point assays were performed at 25 °C as previously described (*9*). A stock solution of substrate contained 50 mM $MgCl_2$ and 20 mM GTP. A 10 mM DEA/NO solution was prepared in 10 mM NaOH. Stock solutions of 1 M nitrosoalkane and 15 mM YC-1 were prepared in DMSO. A 0.5 M dithionite stock solution in H_2O was prepared as described above. A Teflon-sealed Reacti-Vial was filled with CO (Praxair, Inc.). Nitrosoalkanes were generated by adding 10 μL of dithionite to 10 μL of nitroalkane using a gastight syringe immediately before the addition of nitrosoalkane to the assay mixture. Assay mixtures contained 0.2 μg of sGC, 50 mM HEPES (pH 7.4), and 150 μM YC-1 where indicated. In assays with NO, a DEA/NO solution was added to a final concentration of 100 μM. For assays with CO, a gas-tight syringe was used to deliver 10 μL of CO gas to the enzyme. Where indicated, 2 μL of the nitrosoalkane stock solutions was added to the enzyme. Nitroalkane reduction proceeded for 3 min, which was sufficient to saturate the sGC heme with nitrosoalkane. sGC assays were initiated by the addition of $MgCl_2$ and GTP to final concentrations of 2.5 and 1 mM, respectively. All assays were in 1.5 mL eppendorfs in a final volume of 100 μL and contained 2% DMSO, which was shown not to affect enzyme activity. Reactions were quenched after 3 min by the addition of 400 μL of 125 mM $Zn(CH_3CO_2)_2$ and 500 μL of 125 mM Na_2CO_3. cGMP quantification was carried out using a cGMP enzyme immunoassay kit, Format B (Biomol), per the manufacturer's instructions. Each experiment was repeated three times to ensure reproducibility.

RESULTS

Binding of Nitrosoalkanes to Mb, Hb, β1(1−194), and sGC. Nitrosoalkanes were generated *in situ* by the reduction of nitroalkane with dithionite. The combination of nitroalkane and dithionite caused a shift in the Soret absorbance maxima of Mb, Hb, β1(1−194), and sGC. Nitroalkanes or dithionite alone did not change the electronic absorption spectra of the proteins that were examined. The spectra of ferrous sGC and sGC in complex with nitrosopentane are shown in Figure 2. The peak positions of Mb, Hb, β1(1−194), and sGC complexes with nitrosomethane, nitrosopentane, nitrosooctane, and NO are reported in Table 1. All of the nitrosoalkanes that were examined, including nitrosopropane, nitrosobutane, and nitrosohexane, form complexes with absorbance maxima at 425 nm with sGC and at 424 nm with β1(1−194). These results are very similar to those previously reported for the sGC−nitrosomethane complex (*17*). Distinct among the Soret values in Table 1 are the nitrosyl complexes

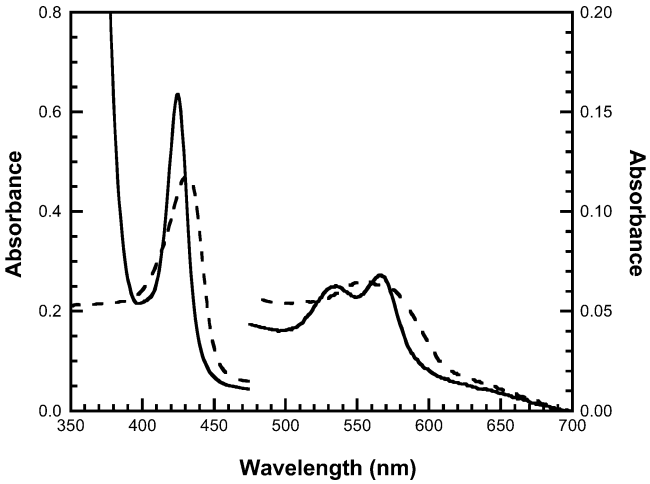

FIGURE 2: Electronic absorption spectra of sGC (3 μM, dashed line) and the sGC−nitrosopentane complex (3 μM, solid line).

Table 1: Electronic Absorption Peak Positions for NO and RNO Bound to Various Heme Proteins[a,b]

protein	ligand	Soret	α/β	ref
Hb	NO	418	574/545	*15*
Mb		423	575/543	*47*
sGC		399	572/537	*1*
β1(1−194)		400	570/537	*8*
Hb	nitrosomethane	421	562/544	*15*
Mb		425	576/547	*15*
sGC		425	568/542	*17*
β1(1−194)		424	565/535	this work
Hb[c]	nitrosopentane	421	565/540	this work
Mb		425	572/540	this work
sGC		425	566/536	this work
β1(1−194)		424	565/536	this work
Hb[c]	nitrosooctane	421	562/540	this work
Mb[c]		425	567/548	this work
sGC		425	568/538	this work
β1(1−194)		424	567/537	this work

[a] All peak positions are in nanometers. [b] Nitroalkane (10 mM) and dithionite (5 mM) unless otherwise noted. [c] Nitroalkane (50 mM) and dithionite (50 mM).

of sGC and β1(1−194) at ∼399 nm, which are five-coordinate complexes. The electronic absorption spectral characteristics of sGC−nitrosoalkane complexes suggest that all the ligands bind to the heme to form six-coordinate, low-spin complexes, similar to Mb− and Hb−nitrosoalkane complexes. Unlike the Soret absorbance maxima, the α and β bands of sGC−nitrosoalkane complexes are sensitive to variations in the nitrosoalkane alkyl chain length.

The binding of all the nitrosoalkanes to sGC and β1(1−194) (∼500 nM) was complete within 1−5 min at 25 °C. In contrast, binding of nitrosoalkane to globins is relatively slow; the larger nitrosoalkanes took 30−60 min to saturate Hb and Mb (1 μM). As the nitrosoalkane chain length increased, the concentration of nitroalkane and dithionite needed to saturate the globin hemes also increased (Table 1). At 10 mM nitroalkane and 5 mM dithionite, nitrosooctane saturates sGC and β1(1−194), but not Mb or Hb. To saturate the globin hemes, it was necessary to increase the concentrations of nitrooctane and dithionite to 50 mM.

Resonance Raman Spectroscopy of the β1(1−194)−Nitrosopentane Complex. Resonance Raman spectroscopy was used to gain further insight into the sGC heme environment, and to confirm the ligation state of the sGC−

Table 2: Resonance Raman Frequencies and Mode Assignments for Various Heme Proteins[a]

protein	ligand	coord	ν_{10}	ν_2	ν_3	ν_4	ν(Fe−N)	ref
Mb	unligated	5	1607	1563	1471	1357		*48*
β1(1−194)		5	1608	1568	1476	1359		*8*
sGC		5	1606	1562	1471	1358		*21*
Mb	NO	6	1638	1584	1501	1375	554	*49*
β1(1−194)		5	1647	1586	1510	1376	526	*8*
sGC		5	1646	1584	1509	1375	525	*21*
Mb	nitrosopentane	6	1639	1583	1505	1375	553	this work
β1(1−194)		6	1630	1580	1499	1372	546	this work
sGC		6	1630	1580	1499	1374	543	this work
Mb	nitrosomethane	6	1636	1586	1500	1373		this work
β1(1−194)		6	1630	1582	1502	1375		this work

[a] Vibrations in cm^{-1}.

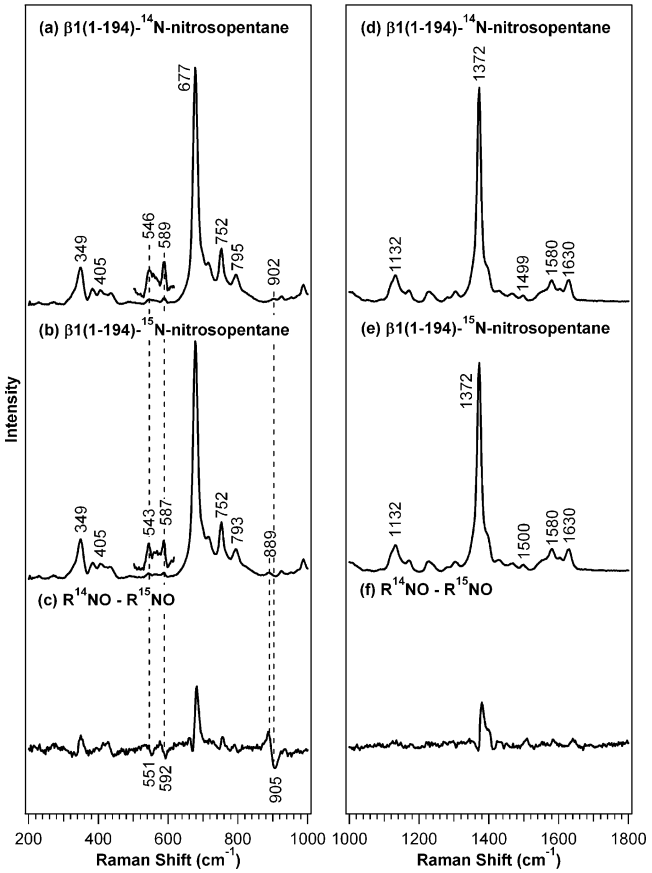

FIGURE 3: Low- and high-frequency resonance Raman spectra of the β1(1−194)−nitrosopentane complex. Spectra obtained with 413.1 nm excitation at 10 °C: β1(1−194)−[^{14}N]nitrosopentane complex (a and d), β1(1−194)−[^{15}N]nitrosopentane complex (b and e), and difference spectra of β1(1−194)−nitrosopentane complex (c and f). The heme concentration was 20 μM. The subtraction factor in the isotopic difference spectra was adjusted to minimize features from vibrational modes that are insensitive to isotopic substitution.

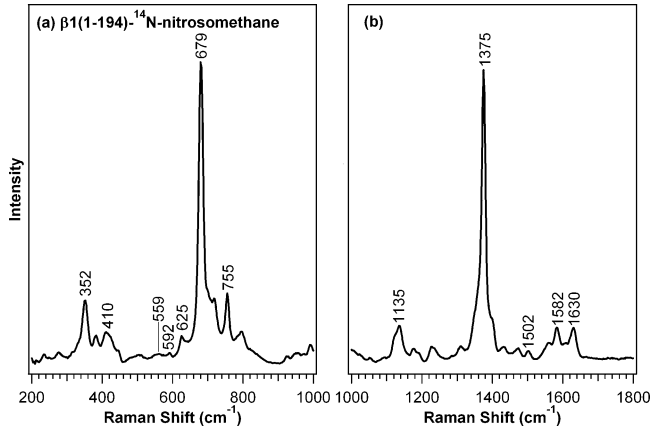

FIGURE 4: Resonance Raman spectrum of the β1(1−194)−nitrosomethane complex. Spectra were obtained with 413.1 nm excitation at 10 °C: low- and high-frequency spectra (a and b, respectively) of the β1(1−194)−[^{14}N]nitrosomethane complex (20 μM).

nitrosoalkane complexes. The oxidation state of the heme iron is indicated by the electron density marker, ν_4, while ν_2, ν_3, and ν_{10} are the spin and coordination state markers (*20*). Table 2 summarizes the heme skeletal marker assignments for unligated and NO/RNO-bound Mb, β1(1−194), and sGC. In the high-frequency spectrum of the β1(1−194)−nitrosopentane complex (Figure 3d), heme skeletal vibrations ν_2, ν_3 and ν_4 and ν_{10} are observed at 1580, 1499, 1372, and 1630 cm^{-1}, respectively, indicating that nitrosopentane binds to β1(1−194) to produce a six-coordinate, low-spin ferrous heme complex (*21*).

Comparison of the low-frequency spectra of [^{14}N]- and [^{15}N]nitrosopentane bound to β1(1−194) (Figure 3a,b) shows that bands at 546, 589, and 902 cm^{-1} are sensitive to isotope substitution. The weakly isotope-sensitive band at 546 cm^{-1} in the β1(1−194)−nitrosopentane complex can be assigned to the Fe−N stretch, based on its similarity to ν(Fe−NO) for previously reported six-coordinate heme−NO complexes (554−558 cm^{-1}) (*22*). This band shifts to 543 cm^{-1} with isotopic substitution, which is in agreement with an expected shift of 4 cm^{-1}. The resonance Raman band at 902 cm^{-1} is assigned to the C−N stretching vibration based on the ν(C−N) for nitromethane (918 cm^{-1}) (*23*). This band shifts to 889 cm^{-1} with isotope substitution, which is also in agreement with the expected shift (14 cm^{-1}). The band at 590 cm^{-1}, which with isotopic substitution shifted to 587 cm^{-1}, is evidently coupled to the Fe−N stretch.

Resonance Raman Spectroscopy of the β1(1−194)−Nitrosomethane Complex. To examine the effect of alkyl chain length on the resonance Raman spectrum, the β1(1−194)−nitrosomethane complex was studied. When nitrosomethane is bound to β1(1−194) (Figure 4b), ν_2, ν_3 and ν_4 and ν_{10} are observed at 1582, 1502, 1375, and 1630 cm^{-1}, respectively. The vibrational frequency of these skeletal markers indicates that nitrosomethane binds to β1(1−194) to form a six-coordinate, low-spin complex. The low-frequency spectrum of this complex (Figure 4a) shows a broad band at 559 cm^{-1} and a band at 592 cm^{-1} which we think are coupled to the Fe−N stretch for the β1(1−194)−

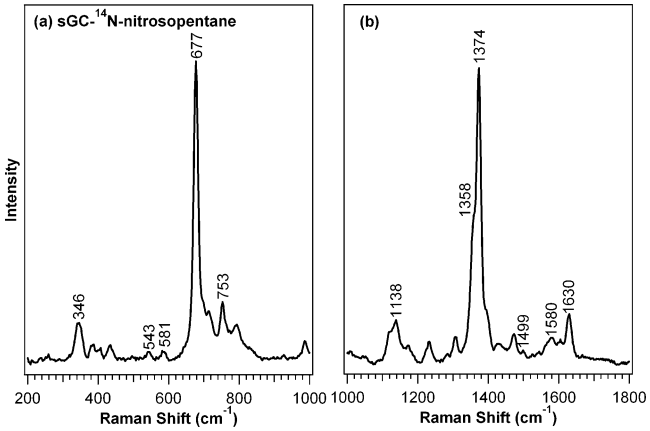

FIGURE 5: Resonance Raman spectrum of the sGC−nitrosopentane complex. Spectra were obtained with 413.1 nm excitation at 10 °C: low- and high-frequency spectra (a and b, respectively) of the sGC−[^{14}N]nitrosopentane complex (5 μM).

nitrosomethane complex based on isotopic studies carried out with the β1(1−194)−nitrosopentane complex (this work) and previously reported assignments for six-coordinate heme−NO complexes (*22*). These bands are at a higher frequency for the β1(1−194)−nitrosomethane complex than for the β1(1−194)−nitrosopentane complex. Comparison of the low-frequency spectrum of this complex (Figure 4a) with that of the β1(1−194)−nitrosopentane complex (Figure 3a) shows the appearance of a new band at 625 cm^{-1} with a decrease in alkyl chain length. The band is present in the spectra of Mb−nitrosomethane and Hb−nitrosomethane complexes at 628 (this work) and 631 cm^{-1} (*16*), respectively. While this band was previously assigned to the Fe−N stretch of the Hb−nitrosomethane complex (*16*), we believe that the band is coupled to the C−N stretch of the ligand. However, further experiments with isotopically labeled nitrosomethane would be necessary to confirm these assignments.

Resonance Raman Spectroscopy of sGC−Nitrosopentane Complexes. The resonance Raman spectra of the sGC−nitrosopentane complex and the β1(1−194)−nitrosopentane complex are very similar. In the high-frequency spectrum of the sGC−nitrosopentane complex (Figure 5b), ν_2, ν_3 and ν_4 and ν_{10} are observed at 1580, 1499, 1374, and 1630 cm^{-1}, respectively. The band at 1374 cm^{-1} has a shoulder at 1358 cm^{-1}, indicating a small amount of photolysis product (*21*). The position of these resonance Raman bands confirms that the complex is six-coordinate and that the heme iron is ferrous. The low-frequency spectrum of the sGC−nitrosopentane complex (Figure 5a) suggests that the vibrational frequency of the Fe−N stretching mode is 543 cm^{-1}. An electronic absorption spectrum of the sGC−nitrosopentane complex collected after resonance Raman data acquisition showed that the Soret peak was slightly broader after exposure to the laser. The change in peak shape was due to laser photolysis, which produced a small population of unligated sGC. The population of unligated protein was shown by resonance Raman and electronic absorption spectroscopy to be dependent on laser power (data not shown).

sGC−Nitrosoalkane Observed Off-Rates. In aqueous solution, nitrosoalkanes will rapidly tautomerize to oximes and dimerize, resulting in products which are not heme ligands

Table 3: Comparison of the Observed Off-Rates from sGC for Various Nitrosoalkanes

ligand	obs k_{off} ($\times 10^{-3}$ s^{-1})	ref
nitrosomethane[a]	22.8 ± 0.6	*17*
nitrosopropane	4.99 ± 0.34	this work
nitrosobutane	1.82 ± 0.0089	this work
nitrosopentane	0.567 ± 0.014	this work
nitrosohexane	0.527 ± 0.028	this work
nitrosooctane	0.111 ± 0.0015	this work

[a] Rate adjusted from 10 to 25 °C by doubling the value for every 10 °C increase in temperature.

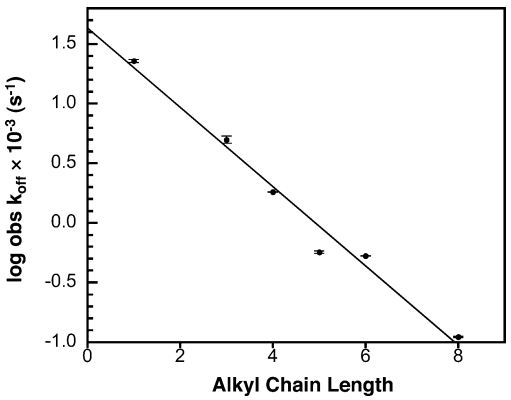

FIGURE 6: Plot of the observed nitrosoalkane off-rates (obs k_{off}) vs nitrosoalkane alkyl chain length. The data were fit to a linear equation (black line) to obtain a slope of −0.33, a *y*-intercept of 1.3, and an R^2 of 0.979.

(*15*). When a nitrosoalkane off-rate from sGC is measured, rebinding of ligand to the heme is in competition with tautomerization and dimerization, leading to the measurement of an observed off-rate (obs k_{off}). The rates of nitrosoalkane tautomerization and dimerization have not been measured. However, it is known that aliphatic nitrosoalkanes exist mainly as dimers in solution, and the rates of dimerization are very rapid such that the nitrosoalkane ligand must be generated *in situ.* As a consequence, it is possible, but unlikely, that the observed rates are influenced by the rates of nitrosoalkane tautomerization and dimerization. The data indicate that the observed off-rates of nitrosoalkanes from sGC are dependent on the nitrosoalkane alkyl chain length. As the alkyl chain length increased from one to eight carbons, the rate decreased from 22.8 × 10^{-3} to 0.111 × 10^{-3} s^{-1} (Table 3). A plot of the log(obs k_{off}) versus nitrosoalkane alkyl chain length reveals a linear correlation (Figure 6). With the assumption that the nitrosoalkane on-rates do not vary with increasing alkyl chain length, the slope of the line, −0.33, can be used to obtain a value of 0.46 kcal of binding energy per carbon in the alkyl chain ($\Delta G = -RT\ln K$).

Activation of sGC by Nitrosoalkanes and YC-1. sGC activity was evaluated in the presence of various nitrosoalkanes at 25 °C (Table 4). With the specified experimental conditions, all nitrosoalkanes fully saturated the sGC heme. Nitrosoalkanes activate sGC 2−6-fold, which is similar to the activation of sGC by CO. sGC activation in the presence of nitrosoalkane and YC-1 was synergistic (Figure 7). In the presence of YC-1, the activation of the sGC−nitrosoalkane complexes was greatest for nitrosopropane and nitrosobutane (45−47-fold), and decreased as alkyl chain length increased, resulting in 11-fold activation by nitrosooctane and YC-1.

Table 4: Activity of sGC Heme Complexes[a,b]

	specific activity (nmol min^{-1} mg^{-1})		fold activation	
ligand	− YC-1	+ YC-1	− YC-1	+ YC-1
−	25 ± 6	69 ± 18	1	3
NO	3107 ± 570	5176 ± 196	127	211
CO	37 ± 17	2835 ± 496	2	115
nitrosopropane	38 ± 3	1093 ± 340	2	45
nitrosobutane	145 ± 11	1156 ± 16	6	47
nitrosopentane	51 ± 14	952 ± 104	2	39
nitrosohexane	60 ± 19	812 ± 158	2	33
nitrosooctane	47 ± 9	281 ± 64	2	11

[a] Values for sGC determined at 25 °C. [b] The concentration of YC-1 was 150 μM.

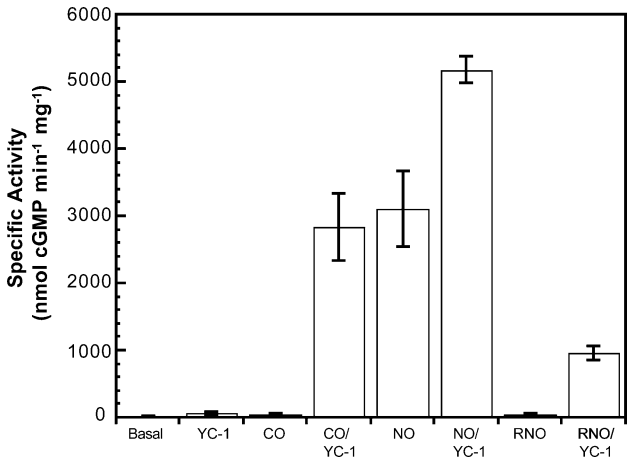

FIGURE 7: Synergistic activation of sGC heme complexes with YC-1. Activity assays of NO−, CO−, and nitrosopentane (RNO)−sGC complexes (0.2 μg) with and without YC-1 (150 μM) at 25 °C.

DISCUSSION

This work establishes nitrosoalkanes (RNO) as a class of sGC heme ligands. The ability of these compounds to activate sGC demonstrates that nitrosoalkanes are also a novel group of enzyme activators. All sGC−nitrosoalkane complexes are characterized by a Soret absorbance maximum at 425 nm, like Mb−nitrosoalkane complexes, suggesting that nitrosoalkanes bind to sGC to form six-coordinate, low-spin complexes. The only variation in the electronic spectra of sGC−nitrosoalkane complexes is in the α and β bands. Similar variations in the α and β band positions are also seen with myoglobin and hemoglobin complexes with nitrosoalkanes (*15*).

The resonance Raman studies presented in this work indicate that the Fe−N stretch for six-coordinate sGC−nitrosoalkane complexes is lower than those of Mb−NO and Mb−nitrosopentane complexes (Table 2). Nitrosomethane and nitrosopentane complexes with β1(1−194) also exhibit ν(Fe−N) at a lower frequency than the respective Mb−nitrosoalkane complexes. The lower ν(Fe−N) for sGC and the sGC heme domain compared to that of Mb likely results from differences in the distal or proximal heme binding pockets of the proteins (*24*, *25*). For example, a hydrogen bond donor within the heme distal pocket appears to be present in globins, but not in sGC or β1(1−194) (*26*). In addition to distal pocket character, ν(Fe−N) is predicted to be sensitive to the Fe−N−O bond angle of NO on the basis of density functional theory (DFT) calculations (*24*, *27*). For binding of NO to heme proteins, ν(Fe−N) decreases as the Fe−N−O angle and the tilting angle decrease. Therefore, the lower ν(Fe−N) in β1(1−194) and sGC when compared to those of the respective Mb−nitrosoalkane complexes could be due to differences in the heme pocket environment and/or the geometry of the ligand.

Nitrosoalkane activation of sGC is independent of alkyl chain length; however, the heme conformation is sensitive to nitrosoalkane size. Comparison of the low-frequency resonance Raman spectra of nitrosopentane and nitrosomethane bound to β1(1−194) shows that some of these bands are also sensitive to nitrosoalkane alkyl chain length. Bands at 435, 405, 383, 349, 271, and 229 cm^{-1} in the β1(1−194)−nitrosopentane complex shift to 444, 410, 383, 352, 276, and 234 cm^{-1}, respectively, in the β1(1−194)−nitrosomethane complex. Bands at comparable frequencies in Mb are similarly affected. Rigorous assignment of these bands would require a comparison of shifts between deuterated and nondeuterated hemes bound to a nitrosoalkane. However, on the basis of work with heme substitutions in metmyoglobin, the bands were tentatively assigned to $\delta(C_\beta C_a C_b)_2 + \delta(C_\beta Me)$, $\delta(C_\beta C_a C_b)_4 + \delta(C_\beta Me)$, $\delta(C_\beta C_c C_d)$, ν_8, ν_{52}, and ν_{24}, respectively (*28*). These bands are sensitive to vinyl, propionate, and/or pyrrole deformations; changing the alkyl length of the nitrosoalkane must therefore influence the environment around these groups in β1(1−194) and Mb. In the resonance Raman spectrum of the sGC−CO complex, similar low-frequency heme bands have been shown to be sensitive to the presence of YC-1 (*29*, *30*). These effects of YC-1 are thought to be related to the YC-1 mechanism of activation; however, our observations suggest that a direct connection between changes in these bands does not necessarily correlate with changes in sGC activity.

Although the nitrosoalkane binding rates could not be measured because the ligands are generated *in situ*, a qualitative comparison of binding of nitrosoalkane to globins and sGC can be made. At any given concentration of nitrosoalkane, binding to the globins is slower than binding to sGC. Also, increased concentrations of nitroalkane and dithionite are needed to saturate the globin hemes relative to the sGC heme. It is important to note that the observed rate of binding of nitrosoalkane to sGC may be limited by the rate of reduction of nitroalkane by dithionite, not binding of nitrosoalkane to the sGC heme. As a consequence, the actual on-rates of nitrosoalkane binding to sGC could be much faster than the values suggested by the reported observed rates. The dependence of both the rate and the extent of nitrosoalkane complex formation on alkyl chain length in globins is similar to that reported for the binding of various isocyanides to globins (*15*), and is thought to be due to the influence of steric hindrance on ligand association rates (*31*−*33*). The fact that this trend is not observed for sGC suggests that the heme has a large distal pocket relative to Mb and Hb.

Nitrosomethane has a relatively fast off-rate from sGC when compared to the globins. In fact, the off-rates of nitrosoalkanes from the globins are so slow that binding is considered irreversible (*15*). The structure of nitrosoethane bound to myoglobin provides an explanation for the stability of these nitrosoalkane−globin complexes, revealing a hydrogen bond between the nitrosoalkane oxygen and the distal

pocket His64 (*34*). The relatively fast off-rate of nitrosomethane from sGC, compared to the irreversible binding of the ligand to the globins, indicates that the presence of a similar hydrogen bond donor in the sGC heme distal pocket is unlikely. In fact, a homology model of β1(1−194) based on the structure of *Tt*Tar4H, the sGC-like heme-binding domain from *Thermoanaerobacter tengcongensis*, shows that there is no hydrogen bond donor in the distal heme binding pocket (*8*). Further information about the sGC heme distal pocket can be obtained from observed nitrosoalkane off-rates by using a quantitative structure−activity relationship (QSAR) analysis. A linear relationship exists between the log(obs k_{off}) of sGC−nitrosoalkane complexes and the alkyl chain length of the nitrosoalkane ligands (Figure 6). Similar linear relationships have been characterized for other proteins and are thought to be a result of the reduction in the number of hydrocarbon−water interactions that occur when the ligand binds to a hydrophobic environment (*35*). A value of 0.46 kcal of binding energy per alkyl chain carbon is obtained from the analysis, in good agreement with a value obtained by plotting octanol−water partitioning coefficients versus alkyl chain length for similar aliphatic alcohols (0.56 kcal/carbon) (*36*, *37*). The agreement between the partitioning of nitrosoalkanes between buffer and the sGC heme and the partitioning of alcohols between water and octanol suggests that the nonpolar alkyl chains of the nitrosoalkanes are removed from water and stabilized by the hydrophobic microenvironment of the sGC heme distal pocket. This information suggests that relatively large, hydrophobic molecules could be designed to target the sGC heme distal pocket for the modulation of enzyme activity.

The QSAR study has implications for theories about the ability of sGC to discriminate between O_2 and NO. Three proposed mechanisms by which sGC may reduce O_2 affinity are a negatively charged distal pocket (*21*, *38*), a sterically constrained distal pocket (*21*, *38*), and the absence of a hydrogen bond donor in the distal pocket (*26*, *39*). Recent work has shown that the introduction of a hydrogen bond donor into the distal pocket of β1(1−385) stabilizes binding of O_2 to the heme (*39*), suggesting that the absence of a hydrogen bond donor in the distal heme pocket is the critical factor for ligand discrimination. The results of the QSAR study reported here demonstrate that sGC has a large hydrophobic heme distal pocket. In addition to excluding a sterically constrained distal pocket as a means of ligand discrimination, this result also supports the proposal that the distal pocket lacks a hydrogen bond donor that could stabilize O_2 and nitrosoalkane binding.

It has been proposed that distal pocket accessibility determines the heme−NO coordination number in cytochromes *c*′ (*40*). In this model, steric hindrance in the distal heme pocket leads to a distorted Fe−N−O geometry and this causes a six-coordinate NO complex to convert to a five-coordinate NO complex where NO binds to the proximal side of the heme. This model has been extended to sGC (*40*, *41*); however, our work demonstrating the presence of a large distal pocket suggests that steric constraint is not a mechanism for controlling the heme−NO coordination number or the location of the bound NO for sGC.

It has been reported that the presence of substrate increases the off-rate of NO from sGC (*18*, *42*, *43*). However, substrate did not affect the observed off-rate of nitrosopentane from the enzyme. YC-1 has been reported to decrease the off-rate of NO from sGC (*44*). On the basis of this result, it was proposed that part of the YC-1 mechanism of activation was to sensitize the enzyme toward NO. When the observed off-rate of nitrosopentane from sGC was monitored, no change was observed with the addition of YC-1 to the sGC−nitrosopentane complex. Thus, when YC-1 binds to the sGC−nitrosopentane complex, the mechanism of activation does not involve a reduction in the ligand off-rate.

Our results indicate that nitrosoalkanes are a novel class of sGC heme ligands that activate the enzyme. Nitrosoalkanes, which are effectively alkyl-substituted NO compounds, activate sGC to the same extent that CO does (Table 4), and like CO, nitrosoalkanes bind to sGC to form six-coordinate complexes. The weaker activation of sGC by nitrosoalkanes when compared to NO emphasizes the unique ability of this gas to activate the enzyme with a mechanism that remains to be elucidated. There is no distinct correlation between nitrosoalkane activation of sGC and the alkyl chain length of the ligand. Nitrosobutane activated sGC to a greater extent than the other nitrosoalkanes (6-fold vs 2-fold), but the reason for this increased level of activation when compared to those of the other nitrosoalkanes is unclear. It is possible that binding of nitrosobutane to sGC leads to a unique conformation which has an enhanced enzyme activity.

All the nitrosoalkanes used in this study activate sGC synergistically with YC-1, with a dependence on nitrosoalkane size. As the alkyl chain length increases from nitrosobutane to nitrosooctane, there is a decrease in the extent of nitrosoalkane/YC-1 activation of sGC. It is possible that the longer alkyl chains interfere with the YC-1 activation mechanism, the details of which are currently unknown. It has been suggested that the binding of YC-1 to a sGC−ligand complex weakens the proximal Fe−His bond and shifts a six-coordinate species to a mixture of six- and five-coordinate species (*29*, *30*, *45*, *46*). In our studies, YC-1 did not affect the coordination state of the sGC−nitrosoalkane complex, as the electronic spectrum of the complex was unchanged by the addition of YC-1. However, the dependence of YC-1 activation on nitrosoalkane chain length provides further support for the connection between the sGC heme and the YC-1 mechanism of action. Furthermore, the synergism of YC-1 with nitrosoalkanes suggests that the mechanism of activation of YC-1 is general for all heme-based sGC activators.

ACKNOWLEDGMENT

We thank Professor Jack Kirsch for helpful discussion concerning linear free energy relationships, Dr. Jonathan Winger for critical input and providing β1(1−194), Dr. Nathaniel Martin for assistance with the synthesis of [^{15}N]-nitropentane, and the Marletta lab for critical reading of the manuscript.

REFERENCES

1. Denninger, J. W., and Marletta, M. A. (1999) Guanylate cyclase and the NO/cGMP signaling pathway, *Biochim. Biophys. Acta 1411*, 334−350.
2. Warner, T. D., Mitchell, J. A., Sheng, H., and Murad, F. (1994) Effects of cyclic GMP on smooth muscle relaxation, *Adv. Pharmacol. 26*, 171−194.

3. Buechler, W. A., Ivanova, K., Wolfram, G., Drummer, C., Heim, J. M., and Gerzer, R. (1994) Soluble guanylyl cyclase and platelet function, *Ann. N.Y. Acad. Sci. 714*, 151−157.
4. Munzel, T., Feil, R., Mulsch, A., Lohmann, S. M., Hofmann, F., and Walter, U. (2003) Physiology and pathophysiology of vascular signaling controlled by guanosine 3′,5′-cyclic monophosphate-dependent protein kinase [corrected], *Circulation 108*, 2172−2183.
5. Wedel, B., Humbert, P., Harteneck, C., Foerster, J., Malkewitz, J., Bohme, E., Schultz, G., and Koesling, D. (1994) Mutation of His-105 in the β1 subunit yields a nitric oxide-insensitive form of soluble guanylyl cyclase, *Proc. Natl. Acad. Sci. U.S.A. 91*, 2592−2596.
6. Zhao, Y., Schelvis, J. P., Babcock, G. T., and Marletta, M. A. (1998) Identification of histidine 105 in the β1 subunit of soluble guanylate cyclase as the heme proximal ligand, *Biochemistry 37*, 4502−4509.
7. Zhao, Y., and Marletta, M. A. (1997) Localization of the heme binding region in soluble guanylate cyclase, *Biochemistry 36*, 15959−15964.
8. Karow, D. S., Pan, D., Davis, J. H., Behrends, S., Mathies, R. A., and Marletta, M. A. (2005) Characterization of functional heme domains from soluble guanylate cyclase, *Biochemistry* (in press).
9. Winger, J. A., and Marletta, M. A. (2005) Expression and characterization of the catalytic domains of soluble guanylate cyclase: Interaction with the heme domain, *Biochemistry 44*, 4083−4090.
10. Stone, J. R., and Marletta, M. A. (1994) Soluble guanylate cyclase from bovine lung: Activation with nitric oxide and carbon monoxide and spectral characterization of the ferrous and ferric states, *Biochemistry 33*, 5636−5640.
11. Stone, J. R., and Marletta, M. A. (1996) Spectral and kinetic studies on the activation of soluble guanylate cyclase by nitric oxide, *Biochemistry 35*, 1093−1099.
12. Mulsch, A., Bauersachs, J., Schafer, A., Stasch, J. P., Kast, R., and Busse, R. (1997) Effect of YC-1, an NO-independent, superoxide-sensitive stimulator of soluble guanylyl cyclase, on smooth muscle responsiveness to nitrovasodilators, *Br. J. Pharmacol. 120*, 681−689.
13. Friebe, A., Schultz, G., and Koesling, D. (1996) Sensitizing soluble guanylyl cyclase to become a highly CO-sensitive enzyme, *EMBO J. 15*, 6863−6868.
14. Stone, J. R., and Marletta, M. A. (1998) Synergistic activation of soluble guanylate cyclase by YC-1 and carbon monoxide: Implications for the role of cleavage of the iron-histidine bond during activation by nitric oxide, *Chem. Biol. 5*, 255−261.
15. Mansuy, D., Chottard, J. C., and Chottard, G. (1977) Nitrosoalkanes as Fe(II) ligands in the hemoglobin and myoglobin complexes formed from nitroalkanes in reducing conditions, *Eur. J. Pharmacol. 76*, 617−623.
16. Chottard, G., and Mansuy, D. (1977) Resonance Raman studies of hemoglobin complexes with nitric oxide, nitrosobenzene and nitrosomethane: Observation of the metal−ligand vibrations, *Biochem. Biophys. Res. Commun. 77*, 1333−1338.
17. Stone, J. R., and Marletta, M. A. (1995) The ferrous heme of soluble guanylate cyclase: Formation of hexacoordinate complexes with carbon monoxide and nitrosomethane, *Biochemistry 34*, 16397−16403.
18. Cary, S. P., Winger, J. A., and Marletta, M. A. (2005) Tonic and acute nitric oxide signaling through soluble guanylate cyclase is mediated by nonheme nitric oxide, ATP, and GTP, *Proc. Natl. Acad. Sci. U.S.A. 102*, 13064−13069.
19. Ballini, R., Petrini, M., and Rosini, G. (1986) (*Z*)-1-Nitro-3-hexane as (*Z*)-3-hexen-1-yl D1-reagent: Synthesis of (*Z*)-5-octen-2-one and (*Z*)-1,8-undecadien-5-one, *Synthesis*, 849−852.
20. Schelvis, J. P., Zhao, Y., Marletta, M. A., and Babcock, G. T. (1998) Resonance Raman characterization of the heme domain of soluble guanylate cyclase, *Biochemistry 37*, 16289−16297.
21. Deinum, G., Stone, J. R., Babcock, G. T., and Marletta, M. A. (1996) Binding of nitric oxide and carbon monoxide to soluble guanylate cyclase as observed with resonance Raman spectroscopy, *Biochemistry 35*, 1540−1547.
22. Lukat-Rodgers, G. S., and Rodgers, K. R. (1997) Characterization of ferrous FixL-nitric oxide adducts by resonance Raman spectroscopy, *Biochemistry 36*, 4178−4187.
23. Rao, C. N. R. (1969) Spectroscopy of the Nitro Group, in *The Chemistry of the Nitro and Nitroso Groups* (Feuer, H., Ed.) pp 79−135, Interscience Publishers, New York.
24. Coyle, C. M., Vogel, K. M., Rush, T. S., III, Kozlowski, P. M., Williams, R., Spiro, T. G., Dou, Y., Ikeda-Saito, M., Olson, J. S., and Zgierski, M. Z. (2003) FeNO structure in distal pocket mutants of myoglobin based on resonance Raman spectroscopy, *Biochemistry 42*, 4896−4903.
25. Franzen, S., Boxer, S. G., Dyer, R. B., and Woodruff, W. H. (2000) Resonance Raman studies of heme axial ligation in H93G myoglobin, *J. Phys. Chem. B 104*, 10359−10367.
26. Pellicena, P., Karow, D. S., Boon, E. M., Marletta, M. A., and Kuriyan, J. (2004) Crystal structure of an oxygen-binding heme domain related to soluble guanylate cyclases, *Proc. Natl. Acad. Sci. U.S.A. 101*, 12854−12859.
27. Tomita, T., Hirota, S., Ogura, T., Olson, J. S., and Kitagawa, T. (1999) Resonance Raman investigation of Fe−N−O structure of nitrosylheme in myoglobin and its mutants, *J. Phys. Chem. B 103*, 7044−7054.
28. Hu, S. Z., Smith, K. M., and Spiro, T. G. (1996) Assignment of protoheme resonance Raman spectrum by heme labeling in myoglobin, *J. Am. Chem. Soc. 118*, 12638−12646.
29. Pal, B., and Kitagawa, T. (2005) Interactions of soluble guanylate cyclase with diatomics as probed by resonance Raman spectroscopy, *J. Inorg. Biochem. 99*, 267−279.
30. Martin, E., Czarnecki, K., Jayaraman, V., Murad, F., and Kincaid, J. (2005) Resonance Raman and infrared spectroscopic studies of high-output forms of human soluble guanylyl cyclase, *J. Am. Chem. Soc. 127*, 4625−4631.
31. Mathews, A. J., Rohlfs, R. J., Olson, J. S., Tame, J., Renaud, J. P., and Nagai, K. (1989) The effects of E7 and E11 mutations on the kinetics of ligand binding to R state human hemoglobin, *J. Biol. Chem. 264*, 16573−16583.
32. Rohlfs, R. J., Mathews, A. J., Carver, T. E., Olson, J. S., Springer, B. A., Egeberg, K. D., and Sligar, S. G. (1990) The effects of amino acid substitution at position E7 (residue 64) on the kinetics of ligand binding to sperm whale myoglobin, *J. Biol. Chem. 265*, 3168−3176.
33. Rodriguez-Lopez, J. N., Smith, A. T., and Thorneley, R. N. (1997) Effect of distal cavity mutations on the binding and activation of oxygen by ferrous horseradish peroxidase, *J. Biol. Chem. 272*, 389−395.
34. Copeland, D. M., West, A. H., and Richter-Addo, G. B. (2003) Crystal structures of ferrous horse heart myoglobin complexed with nitric oxide and nitrosoethane, *Proteins 53*, 182−192.
35. Kirsch, J. F. (1972) Linear Free Energy Relationships in Enzymology, in *Advances in Linear Free Energy Relationships* (Chapman, N. B., and Shorter, J., Eds.) pp 369−400, Plenum Press, London.
36. Hansch, C., Leo, A., and Hoekman, D. H. (1995) Exploring QSAR, in *Hydrophobic, Electronic, and Steric Constants* (Heller, R. S., Ed.) pp 3−49, American Chemical Society, Washington, DC.
37. McKarns, S. C., Hansch, C., Caldwell, W. S., Morgan, W. T., Moore, S. K., and Doolittle, D. J. (1997) Correlation between hydrophobicity of short-chain aliphatic alcohols and their ability to alter plasma membrane integrity, *Fundam. Appl. Toxicol. 36*, 62−70.
38. Jain, R., and Chan, M. K. (2003) Mechanisms of ligand discrimination by heme proteins, *J. Biol. Inorg. Chem. 8*, 1−11.
39. Boon, E. M., Huang, S. H., and Marletta, M. A. (2005) A molecular basis for NO selectivity in soluble guanylate cyclase, *Nat. Chem. Biol. 1*, 53−59.
40. Andrew, C. R., Kemper, L. J., Busche, T. L., Tiwari, A. M., Kecskes, M. C., Stafford, J. M., Croft, L. C., Lu, S., Moenne-Loccoz, P., Huston, W., Moir, J. W., and Eady, R. R. (2005) Accessibility of the distal heme face, rather than Fe−His bond strength, determines the heme-nitrosyl coordination number of cytochromes c′: Evidence from spectroscopic studies, *Biochemistry 44*, 8664−8672.
41. Marti, M. A., Capece, L., Crespo, A., Doctorovich, F., and Estrin, D. A. (2005) Nitric oxide interaction with cytochrome *c*′ and its relevance to guanylate cyclase. Why does the iron histidine bond break? *J. Am. Chem. Soc. 127*, 7721−7728.
42. Kharitonov, V. G., Russwurm, M., Magde, D., Sharma, V. S., and Koesling, D. (1997) Dissociation of nitric oxide from soluble guanylate cyclase, *Biochem. Biophys. Res. Commun. 239*, 284−286.
43. Russwurm, M., and Koesling, D. (2004) NO activation of guanylyl cyclase, *EMBO J. 23*, 4443−4450.
44. Friebe, A., and Koesling, D. (1998) Mechanism of YC-1-induced activation of soluble guanylyl cyclase, *Mol. Pharmacol. 53*, 123−127.

45. Kharitonov, V. G., Sharma, V. S., Magde, D., and Koesling, D. (1999) Kinetics and equilibria of soluble guanylate cyclase ligation by CO: Effect of YC-1, *Biochemistry 38*, 10699−10706.
46. Li, Z. Q., Pal, B., Takenaka, S., Tsuyama, S., and Kitagawa, T. (2005) Resonance Raman evidence for the presence of two heme pocket conformations with varied activities in CO-bound bovine soluble guanylate cyclase and their conversion, *Biochemistry 44*, 939−946.
47. Romberg, R. W., and Kassner, R. J. (1979) Nitric-oxide and carbon-monoxide equilibria of horse myoglobin and *N*-methylimidazole proto-heme: Evidence for steric interaction with the distal residues, *Biochemistry 18*, 5387−5392.
48. Choi, S., Spiro, T. G., Langry, K. C., Smith, K. M., Budd, D. L., and Lamar, G. N. (1982) Structural correlations and vinyl influences in resonance Raman-spectra of protoheme complexes and proteins, *J. Am. Chem. Soc. 104*, 4345−4351.
49. Tsubaki, M., and Yu, N. T. (1982) Resonance Raman investigation of nitric oxide bonding in nitrosylhemoglobin A and -myoglobin: Detection of bound N−O stretching and Fe−NO stretching vibrations from the hexacoordinated NO-heme complex, *Biochemistry 21*, 1140−1144.

BI0515671